



In vitro, *in silico* and *in vivo* study challenges the impact of bronchial thermoplasty on acute airway smooth muscle mass loss

Igor L. Chernyavsky ^{1,10}, Richard J. Russell^{2,10}, Ruth M. Saunders^{2,10}, Gavin E. Morris³, Rachid Berair², Amisha Singapuri², Latifa Chachi², Adel H. Mansur⁴, Peter H. Howarth⁵, Patrick Dennison⁵, Rekha Chaudhuri^{6,7}, Stephen Bicknell⁶, Felicity R.A.J. Rose⁸, Salman Siddiqui², Bindi S. Brook^{9,11} and Christopher E. Brightling^{2,11}

 @ERSpublications
Bronchial thermoplasty treatment for asthma has unexpected possible mechanisms of action
<http://ow.ly/ZcuE30jsaSa>

Cite this article as: Chernyavsky IL, Russell RJ, Saunders RM, *et al.* *In vitro*, *in silico* and *in vivo* study challenges the impact of bronchial thermoplasty on acute airway smooth muscle mass loss. *Eur Respir J* 2018; 51: 1701680 [https://doi.org/10.1183/13993003.01680-2017].

ABSTRACT Bronchial thermoplasty is a treatment for asthma. It is currently unclear whether its histopathological impact is sufficiently explained by the proportion of airway wall that is exposed to temperatures necessary to affect cell survival.

Airway smooth muscle and bronchial epithelial cells were exposed to media (37–70°C) for 10 s to mimic thermoplasty. *In silico* we developed a mathematical model of airway heat distribution post-thermoplasty. *In vivo* we determined airway smooth muscle mass and epithelial integrity pre- and post-thermoplasty in 14 patients with severe asthma.

In vitro airway smooth muscle and epithelial cell number decreased significantly following the addition of media heated to $\geq 65^\circ\text{C}$. *In silico* simulations showed a heterogeneous heat distribution that was amplified in larger airways, with <10% of the airway wall heated to $>60^\circ\text{C}$ in airways with an inner radius of ~ 4 mm. *In vivo* at 6 weeks post-thermoplasty, there was an improvement in asthma control (measured via Asthma Control Questionnaire-6; mean difference 0.7, 95% CI 0.1–1.3; $p=0.03$), airway smooth muscle mass decreased (absolute median reduction 5%, interquartile range (IQR) 0–10; $p=0.03$) and epithelial integrity increased (14%, IQR 6–29; $p=0.007$). Neither of the latter two outcomes was related to improved asthma control.

Integrated *in vitro* and *in silico* modelling suggest that the reduction in airway smooth muscle post-thermoplasty cannot be fully explained by acute heating, and nor did this reduction confer a greater improvement in asthma control.

This article has supplementary material available from erj.ersjournals.com

Received: Aug 17 2017 | Accepted after revision: March 29 2018

Copyright ©ERS 2018. This ERJ Open article is open access and distributed under the terms of the Creative Commons Attribution Licence 4.0.

Affiliations: ¹School of Mathematics, University of Manchester, Manchester, UK. ²Dept of Infection, Immunity and Inflammation, Institute for Lung Health, NIHR Leicester Biomedical Research Centre, University of Leicester, Leicester, UK. ³Dept of Cardiovascular Sciences, University of Leicester, Leicester, UK. ⁴Heart of England NHS Trust, Birmingham, UK. ⁵Clinical and Experimental Sciences, University of Southampton, Southampton NIHR Respiratory Biomedical Research Unit, University Hospital Southampton NHS Trust, Southampton, UK. ⁶Gartnavel General Hospital, Glasgow, UK. ⁷Institute of Infection, Immunity and Inflammation, University of Glasgow, Glasgow, UK. ⁸Centre for Biomolecular Sciences, University of Nottingham, Nottingham, UK. ⁹School of Mathematical Sciences, University of Nottingham, Nottingham, UK. ¹⁰These authors contributed equally to the study. ¹¹Co-senior authors.

Correspondence: Igor L. Chernyavsky, School of Mathematics, University of Manchester, Oxford Road, Manchester M13 9PL, UK. E-mail: Igor.Chernyavsky@manchester.ac.uk

Introduction

Bronchial thermoplasty (BT) is a non-pharmacological therapy for treating severe asthma by selectively heating conductive airways (3–10 mm in diameter) from within the lumen with a low-power electrical current [1, 2]. During the BT procedure, thermal energy is delivered to the airway wall *via* a bronchoscope-inserted catheter with a distal basket of four electrodes that expand to make contact with the airway wall, aiming to reach a target temperature of 65°C for 10 s.

The primary target of BT is the airway smooth muscle (ASM), a key contributor to airway remodelling, particularly in severe asthma [2–7]. Previous animal studies demonstrated a reduction in airway hyper-responsiveness and an altered ASM histological appearance following BT [8]. Subsequent clinical trials showed improved quality of life and reduced frequency of severe exacerbations in those receiving BT *versus* a sham procedure, but found no significant difference in lung function as a result of the treatment [9–12]. In uncontrolled observational studies, BT has been associated with an ~50–80% relative loss of ASM mass determined by bronchial biopsies [13–16], which were typically obtained 1–3 months after completion of the BT procedures. Although thermal ablation by radiofrequency energy is commonly used in surgical practice [17, 18], there is a paucity of theoretical [19] and *in vitro* [20] studies in humans that assess the direct effect of supra-febrile temperatures on ASM cells' survival and function, or the early effects of BT upon ASM mass and epithelial integrity.

We hypothesised that during BT the proportion of the airway exposed to temperatures necessary to affect ASM and epithelial cell survival, determined from *in vitro* experiments, is sufficient to explain the impact of BT. To test our hypothesis we employed *in vitro*, *in silico* and *in vivo* methodologies to define the acute impact of BT on ASM and epithelial cells.

Methods

Detailed methods are included in the supplementary material.

In vitro heating of human primary ASM, epithelial cells and bronchial epithelial cells

Primary ASM and epithelial cells were cultured as described previously [21]. The study was approved by the Leicestershire Research Ethics Committee (REC 08/H0406/189). Informed consent was obtained from all subjects. The human bronchial epithelial cells (hBECs) were obtained from LGC Standards (Middlesex, UK).

Cells were grown to confluence in 6- or 24-well plates, then exposed to heated media for 10 s using the protocol described in the supplementary methods. Heat loss over the 10-s period was measured and showed that following the addition of media heated to 65°C, cells were exposed to a mean temperature of 58–59°C in both 6- and 24-well plates (supplementary table S4).

The number of remaining adherent viable cells up to 2 weeks post-heating was assessed using PrestoBlue® (Thermo Fisher Scientific, Warrington, UK) according to manufacturer's instructions and confirmed at specified times by cell counts. The percentage of the remaining adherent cell population undergoing apoptosis or necrosis 24 h post-heating was determined using the Alexa Fluor® 488 Annexin V/Dead Cell Apoptosis Kit (Thermo Fisher Scientific) as described previously [22]. Fluorescence emission was collected at 530 nm (Annexin V) and >575 nm (propidium iodide) on a flow cytometer and the percentage of apoptotic and necrotic cells derived respectively using WEASEL™ software (Frank Battye Flow Cytometry Consulting, Melbourne, Australia).

In silico bioheat mathematical modelling

Because it is not currently possible to measure the heat transfer within the airway wall during BT *in vivo*, a two-dimensional mathematical model was developed that couples Joule heating due to the electrical current generated by the BT electrodes (with integrated temperature control feedback, similar to [19]) with

the bioheat transfer in the airway wall and surrounding parenchymal tissue. The material properties of the lung were applied to the model as shown in supplementary table S1. The coupled model was implemented using the finite element-based modelling framework of COMSOL Multiphysics® 5.2 (Stockholm, Sweden). Heat maps were integrated over the airway wall to characterise heating pattern heterogeneity.

Local sensitivity analysis was conducted to identify key geometric, physiological and equipment parameters, and to test the robustness of model predictions. Mathematical model formulation and further technical details can be found in the supplementary material. The mathematical model was validated using the *in vitro* data on the cooling of heated media in multi-well plates (see the *in vitro* methods above), which showed good agreement (supplementary figure S3).

The predicted distribution of temperatures in the airway wall, in combination with the thermal dose-dependent response of ASM and bronchial epithelial cells *in vitro*, was used to estimate the overall acute impact of BT on the bronchial wall (the modelling framework is illustrated in supplementary figure S1).

In vivo response to BT

Bronchial biopsies were obtained from 14 subjects before and after BT. All subjects had severe asthma as defined by American Thoracic Society/European Respiratory Society guidelines, and underwent BT as part of their clinical care.

BT was performed as per manufacturer's guidelines over three staged treatment sessions in the following order: right lower lobe, left lower lobe, and both right and left upper lobes. The right middle lobe was not treated owing to the risk of airway collapse and "right middle lobe syndrome" [23]. Biopsies were obtained from the untreated right upper lobe at the first BT session and the treated right lower lobe segmental and subsegmental airways at the second BT session.

Biopsies were embedded in paraffin and 4- μ m sections stained with haematoxylin and eosin or anti- α -smooth muscle actin (α -SMA, clone 1A4; Dako, Stockport, UK). Biopsies were assessed by a single observer (RJR) blinded to clinical characteristics to determine 1) the ASM content as a percentage of total biopsy area; 2) the epithelial integrity by measuring and expressing the length of intact, damaged and denuded epithelium as a percentage of reticular basement membrane length; and 3) the number of myofibroblasts (isolated α -SMA-positive stained cells in the lamina propria that were neither located as part of the ASM bundle nor as vascular smooth muscle cells adjacent to vessels) per mm² of lamina propria.

Statistical analysis

The statistical analysis is discussed in more detail in the supplementary methods. Briefly, data were analysed in GraphPad Prism® 7.0 and R project 3.2.4, using parametric and non-parametric tests as appropriate. Confidence intervals for the medians of cell counts were estimated using the bootstrap percentile method (R boot package). A p-value <0.05 was considered statistically significant.

Results

In vitro apoptosis and necrosis of ASM and hBEC cells

A metabolic assay demonstrated that the addition of media heated to 65°C or 70°C for 10 s, but not 45–60°C, resulted in a significant reduction in the number of ASM and hBEC cells remaining adherent after 24 h compared to 37°C (figure 1a, b). This reduction in the number of viable (metabolically active) adherent cells persisted over 2 weeks after the addition of media heated to 65°C or 70°C for ASM and to 70°C for hBEC cells compared to 37°C. The number of viable hBEC cells recovered, such that 10 days after the addition of media heated to 65°C their numbers were not significantly reduced *versus* 37°C (figure 1a–d). The results presented in figure 1a–d were confirmed at various times using cell counts (figure 1e, f), which supported the results of the metabolic assay. There was a significant reduction in ASM and hBEC cell counts after the addition of media heated to 65°C at 24–48 h (data not shown), which persisted for 1 week (figure 1e) and 2 weeks (data not shown) for ASM, with a recovery of hBEC cell number after 1 week (figure 1f). In addition to the reduction in ASM and hBEC cell number post-addition of media heated to 65°C or 70°C *versus* 37°C, there was a significant increase in the percentage of cells undergoing necrosis, but not apoptosis (figure 1g, h) in the remaining adherent cell population after 24 h. The median of the relative reduction in viable ASM cell number after the addition of media heated to 65°C at 24 h was 60% (95% bootstrap CI 40–80%).

In silico heating heterogeneity profiles

Our computational finite element-based model implementing the BT protocol showed a high degree of temperature variation over an airway wall. An example with reference model geometry (inner and outer wall radii of 2.2 and 3.3 mm, respectively) is shown in figure 2. To assess the impact each of the parameters in the mathematical model had on heat distribution, we undertook a local sensitivity analysis (supplementary material). This demonstrated that the model predictions were relatively insensitive to the

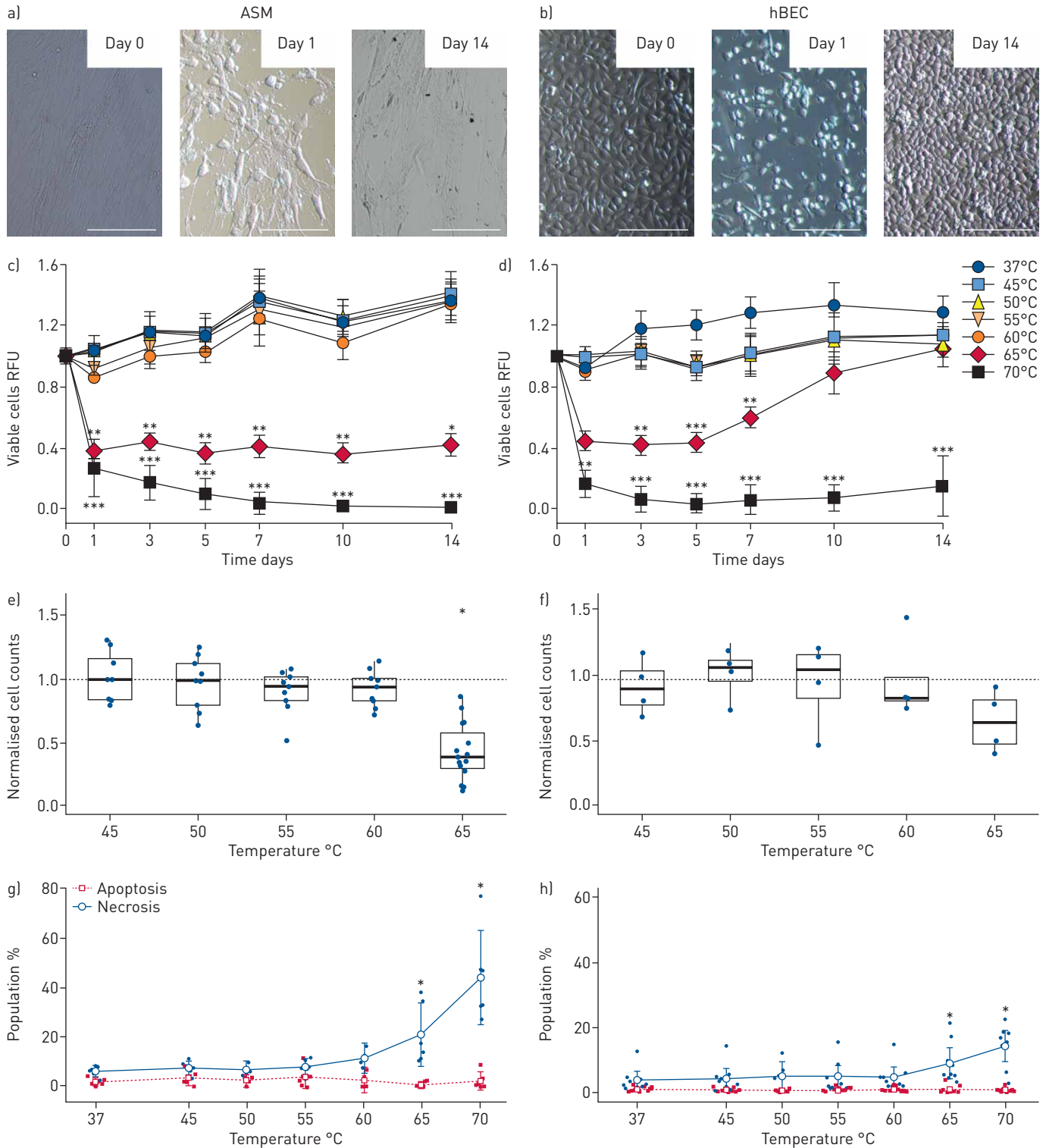


FIGURE 1 Response of *in vitro* heated airway smooth muscle (ASM) and human bronchial epithelial (hBEC) cells. **a, b**) Representative cell morphology for cultures following addition of media heated to 65°C; note the incomplete recovery of ASM **a**) compared to hBEC **b**) cells over 2 weeks. Scale bar, 0.1 mm. **c, d**) Longitudinal viability of ASM **c**) and hBEC **d**) cells following addition of media heated to specified temperatures (mean±SE). **e, f**) Total cell count relative to 37°C-matched control 1 week after the addition of heated media for ASM **e**) and hBEC **f**) cells. **g, h**) Proportion of apoptotic and necrotic ASM **g**) and hBEC **h**) cells determined by flow cytometry 24 h after the addition of media heated to specified temperatures (mean, 95% CI). **p*<0.05, ***p*<0.01, ****p*<0.001 versus 37°C controls.

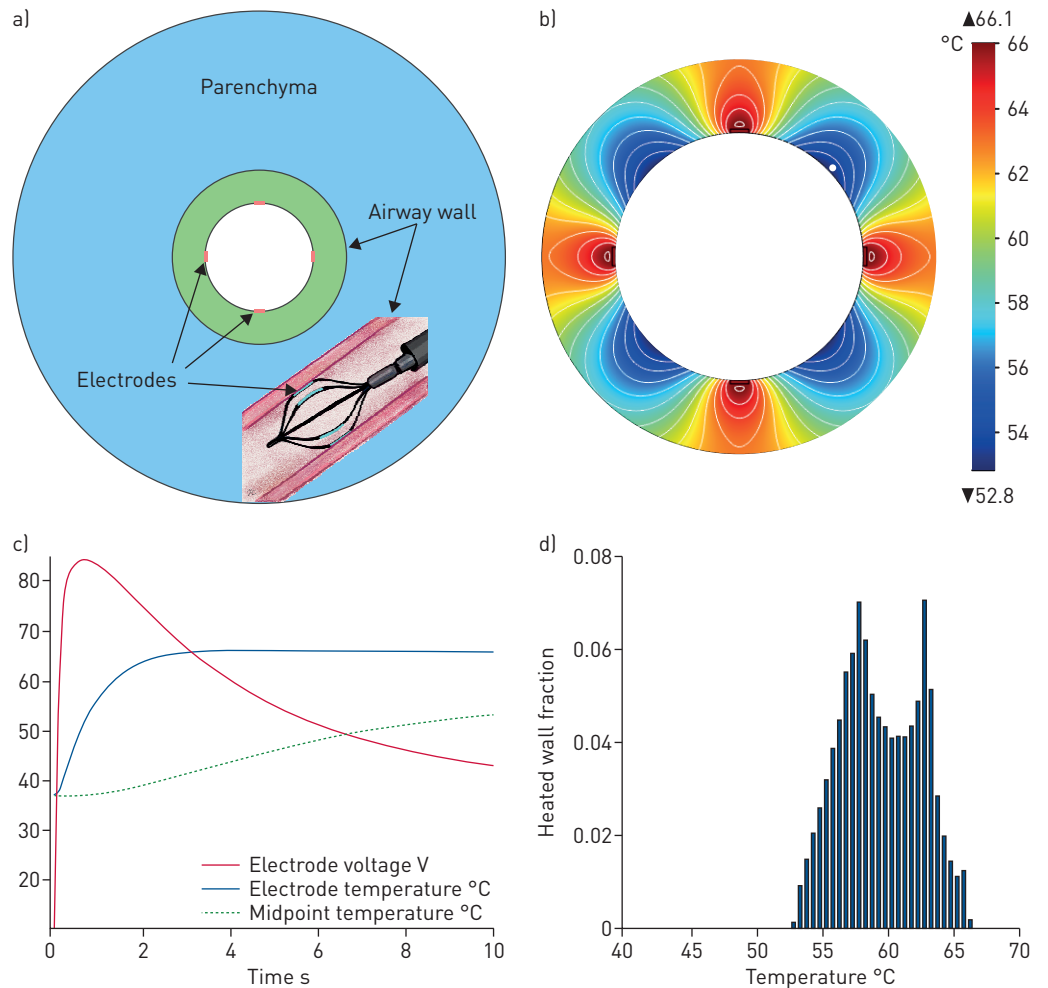


FIGURE 2 Characterisation of bronchial thermoplasty (BT) heating patterns. a) Reference model geometry (inner wall radius of 2.2 mm, outer radius of 3.3 mm). b) Heat map at the end of a single BT activation (10 s). c) Temporal dynamics of the applied voltage (red), electrode temperature (solid blue) and temperature at the midpoint between two electrodes (dashed green; marked by a white dot in b). d) Distribution of heated wall area fractions, corresponding to b.

tissue material properties and heating control parameters (supplementary table S3), but strongly dependent on the airway calibre and wall thickness (supplementary table S3 and figure S2). This amplification of temperature variation in the larger airways is shown in figure 3, demonstrating only a small fraction of the wall heated to 65°C (figure 3 and table 1).

Although energy transfer is more efficient in the smallest airways accessible to a BT catheter (figure 3a), suboptimal heating is possible in the case of an occluded airway with reduced luminal cooling (figure 3b), and heating heterogeneity is strongly exacerbated in larger airways (figure 3c). Our model suggests that <5% of a typical airway (internal radius ~4 mm) treated with BT is exposed to temperatures >65°C, and <10% to temperatures >60°C (table 1). Post-BT thermal equilibration does not improve the extent of heating in the upper temperature range, with no portion of the wall experiencing temperatures >65°C in the 1–2 s after the end of energy delivery (figure 3d, e), even when there is no volumetric cooling due to tissue perfusion and alveolar moisture evaporation. Therefore, only a small percentage of the area of airways treated with BT are likely to be exposed to temperatures >60°C, except for the smallest treated airways. Owing to the accessibility of the airways with a bronchoscope, those airways biopsied were proximal to the smallest airways treated with BT.

In vivo BT impact on ASM mass and epithelial integrity

The baseline and follow-up clinical characteristics of the 14 subjects are shown in table 2. Nine subjects were receiving treatment with regular systemic corticosteroids (Global Initiative for Asthma (GINA) step 5) and the remaining subjects were receiving GINA step 4 treatment. Six weeks after the last BT

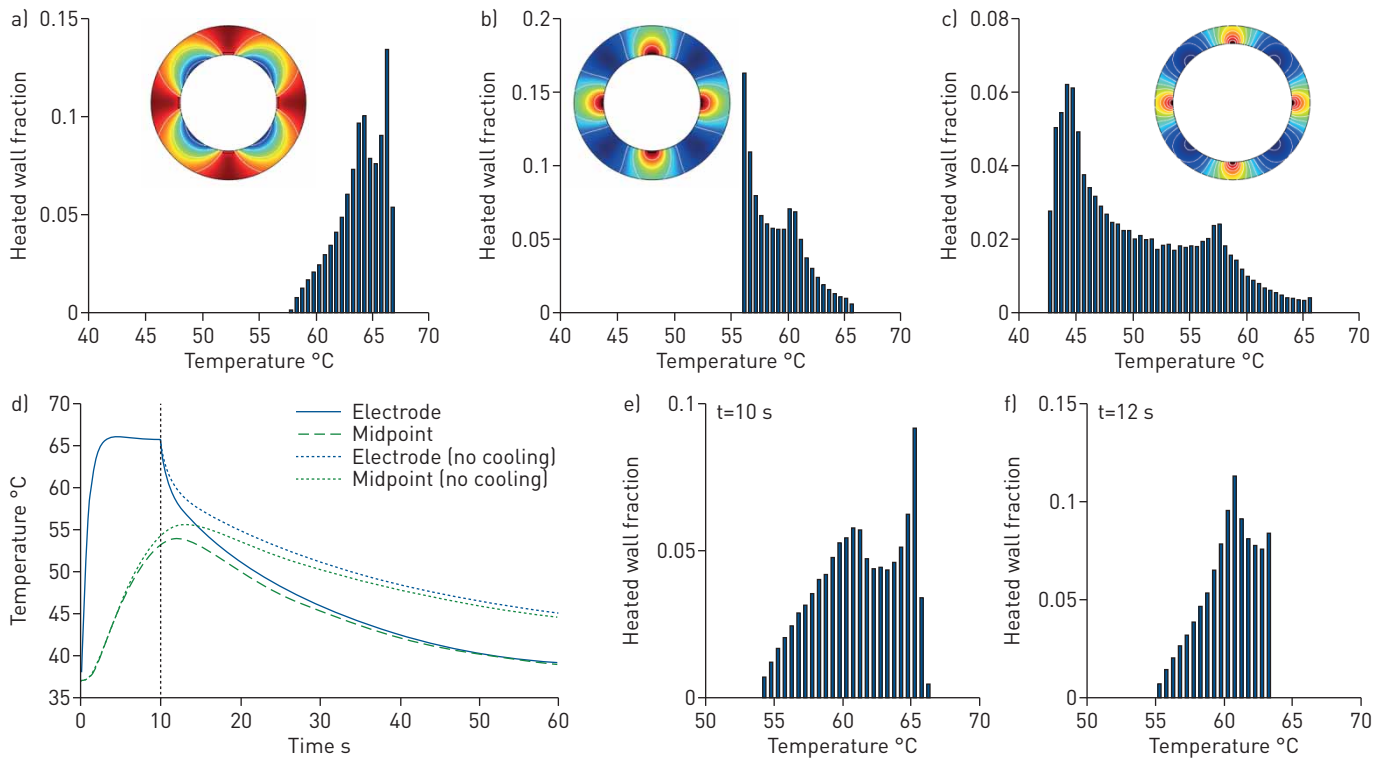


FIGURE 3 Airway temperature heterogeneity across bronchial generations and heating scenarios. Heating patterns a) at the lowest end of bronchial thermoplasty (BT) applicability (luminal radius of 1.5 mm); b) for a midrange airway (luminal radius of 2.2 mm, corresponding to figure 2b, d) with impeded luminal evaporative cooling (e.g. occluded with a bronchoscope); and c) for a larger airway (luminal radius of 4.4 mm). d) Thermal dynamics of an airway wall after the end of a single BT activation (marked by vertical dashed line) for the reference case of figure 2 (solid and dashed) and for the case of absent tissue perfusion and evaporative cooling (dotted lines). e, f) Temperature distributions at 10 s (e) and 12 s (f), corresponding to the case of absent volumetric tissue cooling.

intervention there was no change in lung function, whereas scores for both the Asthma Control Questionnaire-6 (ACQ6) and Asthma Quality of Life Questionnaire (AQLQ) significantly improved by more than the clinically important difference of 0.5 (ACQ6 mean difference -0.7, 95% CI -1.3 to -0.1, p=0.03; AQLQ mean difference 0.8, 95% CI 0.1 to 1.5, p=0.03) (table 2).

The median time between baseline and follow-up biopsies was 28 days (range 14–56 days). A representative bronchial biopsy is shown in figure 4a. There was a reduction in median ASM mass from 12% (interquartile range (IQR) 6–17) pre-BT to 6% (IQR 1–10) post-BT (median difference 5%, IQR 0–10, Wilcoxon p=0.03; figure 4b). The median relative reduction in ASM mass was 58% (IQR 6–90).

There was also a significant improvement in median epithelial integrity from 29% (IQR 15–40) pre-BT to 46% (IQR 25–56) post-BT (median improvement 14%, IQR 6–29, p=0.007; figure 4c, d). The median relative increase in epithelial integrity was 56% (IQR 19–120).

TABLE 1 Quantification of simulated thermal impact of bronchial thermoplasty at the end of an activation cycle

	Intermediate conducting airway [#]		Large conducting airway [¶]
	Baseline	Occluded (no evaporative cooling)	
Mean wall temperature °C	59	59	50
Wall area fraction heated >65°C %	3	2	1
Wall area fraction heated >60°C %	43	35	7
Wall area fraction heated >55°C %	93	100	25

[#]: inner radius 2.2 mm, outer radius 3.5 mm; [¶]: inner radius 4.4 mm, outer radius 5.7 mm.

TABLE 2 Baseline and follow-up (median time of 28 days) clinical characteristics of patients undergoing thermoplasty and biopsy

Characteristic	Baseline	Follow-up	p-value
Subjects n	14	–	
Female sex n	9	–	
Age years	52±13	–	
GINA classification 5 n	9	–	
BMI kg·m ⁻²	31±8	–	
Exacerbations in last 12 months n	4±3	–	
Pre-BD FEV ₁ % predicted	68±19	67±20	0.5
Post-BD FEV ₁ /FVC %	63±12	63±12	0.8
Bronchodilator reversibility %	19±11	16±12	0.5
ACQ6 score	3.1±1.6	2.5±1.7*	0.03
AQLQ score	3.4±1.7	4.1±1.8*	0.03

Data are presented as mean±sd, unless otherwise indicated. GINA: Global Initiative for Asthma; BMI: body mass index; BD: bronchodilator; FEV₁: forced expiratory volume in 1 s; FVC: forced vital capacity; ACQ6: Asthma Control Questionnaire-6; AQLQ: Asthma Quality of Life Questionnaire. *: paired *t*-test *p*<0.05 compared to baseline.

There was a numerical but nonsignificant reduction in the number of sub-epithelial myofibroblasts (pre-BT median 25 cells·mm⁻², IQR 7–47 versus post-BT median 13 cells·mm⁻², IQR 6–21; *p*=0.17). There was a significant inverse correlation between the change in ASM mass and myofibroblast count in the lamina propria following BT (Spearman *r*=−0.55, *p*=0.046; figure 4e). Change in epithelial integrity did not correlate with change in myofibroblast count nor ASM mass following BT (data not shown).

Improvements in AQLQ score did not correlate with pre-BT epithelial integrity, ASM mass or myofibroblast number in the lamina propria nor with post-BT change (data not shown). Only three subjects had an improvement ≥1.0 thus no responder analysis was undertaken. Pre-BT epithelial integrity, ASM mass and myofibroblast number in the lamina propria were not related to change in ACQ6 score (data not shown). The change in ACQ6 score was inversely related to the change in ASM mass (Spearman *r*=−0.67, *p*=0.018), but not with epithelial integrity (*r*=−0.03, *p*=0.09) or myofibroblast number in the lamina propria (*r*=0.41, *p*=0.18). Five subjects had an improvement in ACQ6 score ≥1.0. Compared with subjects not showing this improvement in ACQ6, these five subjects had a small increase in ASM mass post-BT (median 2%, IQR −2 to 8 versus median −10%, IQR −8 to −12; *p*=0.003). This was in contrast to a higher pre-BT myofibroblast number in the lamina propria (59 cells·mm⁻², IQR 36–84 versus 7 cells·mm⁻², IQR 3–43; *p*=0.03) and greater decrease post-BT (37 cells·mm⁻², IQR 30–51 versus −8 cells·mm⁻², IQR 3 to −27; *p*=0.048). Those with both an increase in ASM mass and a decrease in myofibroblast number in the lamina propria had the greatest improvement in ACQ6 score compared with those that either had a decrease in both or a decrease in ASM mass and increase in myofibroblast number (figure 4e).

Discussion

We have developed an integrated *in vitro* and *in silico* framework to model the acute effects of BT on ASM and epithelial cells. In this framework, the *in silico* mathematical model serves as a “bridge” between the *in vitro* and *in vivo* thermal effects, which are inaccessible by other means. The *in vitro* model identified a sharp threshold in the response of both hBEC and ASM cells to heating. *In vitro* hBEC and ASM cell number decreased significantly after the addition of media heated to ≥65°C. Importantly, taking into account the heat loss over 10 s in the *in vitro* experiments, these cells were exposed to a mean temperature of 58–59°C. The mathematical model predicted a localised and highly heterogeneous heating pattern that is very sensitive to airway calibre, with a relatively small fraction of the bronchial wall heated to >60°C in all but the smallest airways (see also [25]). The integrated *in vitro* and *in silico* model predictions were tested against *in vivo* bronchial biopsies taken pre- and post-BT. The biopsy samples showed an increase in epithelial integrity and a reduction in ASM mass after BT.

Although greater than predicted based on our mathematical model, the observed post-BT relative median reduction in ASM mass of 58% was consistent with previous clinical studies [13–16]. To explain this level of ASM reduction by acute thermal injury alone, most of the airway wall in the calibre of airways sampled at bronchoscopy would need to be heated to ≥60°C. Thus, if the *in vitro* and *in silico* predictions are correct, the difference must be due to an alternative biological mechanism triggered in response to BT, such as the active thermal bystander effect [26].

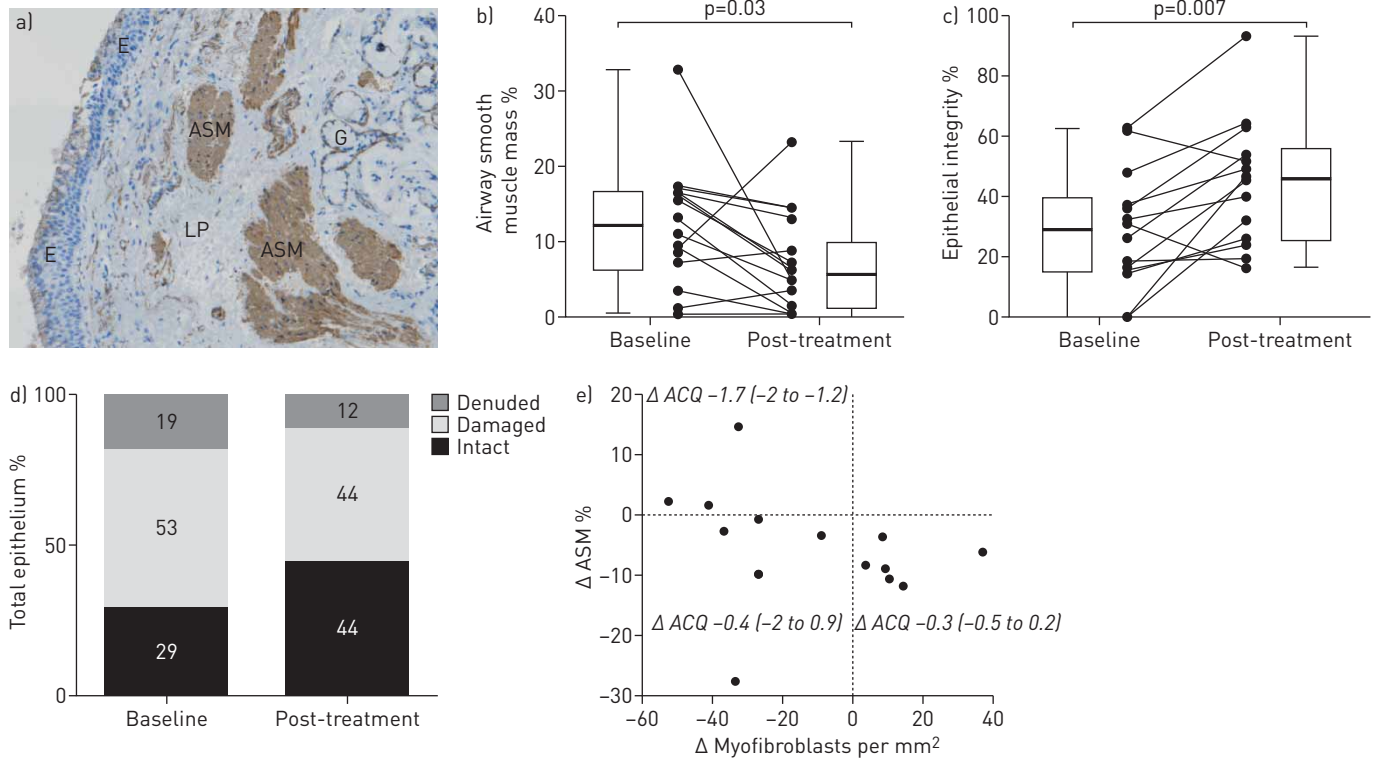


FIGURE 4 Histology analysis of airway smooth muscle (ASM) content and epithelial integrity in bronchial biopsies (at baseline and at about 1 month post-bronchial thermoplasty (BT)). a) Example endobronchial biopsy stained for α -smooth muscle actin (E: epithelium; LP: lamina propria; G: gland). b) ASM mass % pre- and post-BT ($p < 0.05$). c) Epithelial integrity pre- and post-BT ($p < 0.01$). In b and c, the horizontal line represents the median, the box represents the interquartile range (IQR) and the whiskers represent the minimum and maximum. d) Detailed breakdown of epithelial structure at baseline and post-BT (mean). The total percentage for the baseline does not equal 100% owing to rounding. e) Change in ASM mass versus the number of myofibroblasts per mm^2 of lamina propria following BT (Spearman's rank correlation $r = -0.55$, $p = 0.046$), with change in Asthma Control Questionnaire-6 [ACQ6] score [mean (IQR)] reported for each response subgroup (quadrants).

Our *in vivo* biopsies showed significantly improved epithelial integrity after BT, which likely reflects epithelial repair in response to thermal injury. Indeed, our *in vitro* data show evidence of acute phase epithelial repair in response to heat. Others studies have not found changes in the epithelial phenotype in biopsies obtained 3 months after completion of BT treatment, but have reported other effects upon collagen deposition and bronchial nerves [16]. Although in this small study a reduction in ASM mass did not correlate with increased epithelial integrity, whether epithelial repair might impact on other changes in airway wall structure, including ASM mass, following BT warrants further investigation.

Myofibroblast numbers are increased in the lamina propria in patients with asthma and they traffic to sites of injury, differentiate and promote wound repair [27–29]. We considered whether BT might affect the number of myofibroblast cells in the lamina propria, and whether the prevalence of these cells might relate to changes observed in the epithelium and ASM. We identified a numerical but nonsignificant reduction in the overall number of myofibroblasts in the lamina propria in response to BT. However, there was a significant inverse correlation between the change in ASM mass and myofibroblast number after BT. This might represent a dynamic relationship between myofibroblasts and the ASM bundle, with migration of myofibroblasts to and from the ASM bundle. Despite the small number of subjects in our study, we were able to explore the relationship between the effects of BT on ASM mass, epithelial integrity and myofibroblast numbers in the lamina propria and asthma-related symptoms assessed 6 weeks after the last BT intervention. Surprisingly we found that improvement in asthma control was inversely related to post-BT change in ASM mass, and that improvement in asthma control was greatest in those with an increase in ASM mass and a reduction in myofibroblast number. The observed epithelial repair was not associated with improved asthma control, but whether epithelial repair contributes to the reduced exacerbation rates observed in larger studies after BT needs to be further investigated.

Our study had a number of potential limitations. The *in vitro* studies could not fully recapitulate the behaviour of the ASM cells and bronchial epithelial cells *in vivo* because the heated media was added directly to specific cell types in isolation. They also did not take into account asthmatic *versus*

non-asthmatic cellular phenotype, cell–cell interactions or the presence of submucosal tissue. In addition, there was a small amount of heat loss over the 10-s exposure in the model system. However, our *in vitro* data were very consistent across different methodological approaches and between two centres.

The mathematical model involved a number of simplifying assumptions. We modelled an airway and surrounding parenchyma as a cross-section and neglected three-dimensional effects. This approximation is justified by the relatively long (~5 mm) length of the electrode compared to the airway wall thickness (~1 mm). The computational model also used averaged homogeneous electrothermal material properties of the airway wall and parenchymal tissues and did not account for possible anatomic-physiological variations within and between treated individuals. There was also the possibility of inherent operator variability, patient lung movement and complex automatic controller safeguards incorporated into the BT protocol, which were not included in the model. We have, however, tested the robustness of the *in silico* model and quantified the uncertainty associated with model predictions *via* 1) appropriate mesh convergence tests, 2) application of random spatial perturbations in tissue material properties (results not shown) and 3) a comprehensive parameter sensitivity analysis. Indeed, the sensitivity analyses showed that model predictions remained unaffected by a moderate level of variability in tissue material properties, whereas airway wall and luminal morphometry had the greatest impact on the model. Nonetheless, the developed mathematical modelling framework is intended to provide a qualitative rather than quantitative insight into the impact of BT. Thus, notwithstanding the limitations of the *in vitro* and *in silico* modelling, we are confident that these data do not support the concept of substantial acute loss of ASM mass as a direct response to the heating effect of BT in the airways sampled at bronchoscopy.

There were also shortcomings in the BT *in vivo* clinical trial. First, the *in vivo* bronchial biopsies were taken from the right upper lobe at baseline and the right lower lobe following BT, and the ASM mass at baseline was lower than we have previously reported [24]. It is possible that some of the changes demonstrated were due to variability in baseline remodelling between lung lobes, and variability in subject selection in this cohort compared to others. We also observed a high degree of inter-patient variability in the ASM response to BT. However, despite these factors, the observed overall magnitude of ASM mass reduction was similar to that given in previous reports, giving confidence to the likelihood of the observed changes being genuine. Finally, our BT *in vivo* study was too small to determine whether the observed changes in airway remodelling relate to future clinical risk such as exacerbations. Determining this requires either a large prospective study or a meta-analysis of the reported BT biopsy studies.

In conclusion, our *in vivo* data support a reduction in ASM mass in bronchial biopsies obtained post-BT but our combined *in vitro* and *in silico* modelling suggest that the extent of this reduction in ASM mass cannot be entirely explained by a direct acute effect of thermal injury on ASM following BT. Although we cannot exclude the possibility that peri-procedural prednisolone contributed to remodelling, prednisolone was administered prior to all procedures and, importantly, its effects on the epithelium are inconsistent and no effects on the ASM mass have previously been reported [30]. Our data therefore challenge the current concepts of the potential mechanisms of BT, indicating that an alternative mechanism(s) besides direct thermal injury may contribute to this process. Epithelial integrity was also shown to increase in response to BT, and post-BT myofibroblast number in the lamina propria was inversely related to ASM mass. Whether epithelial repair in response to thermal injury and/or the dynamic interaction between the ASM and myofibroblasts have consequent effects upon BT-associated reduced ASM mass remains to be confirmed. Whether the BT protocol can be optimised to target specific airways or elements of airway remodelling, perhaps in combination with patient-specific modelling to facilitate precision medicine, needs to be studied.

Acknowledgements: The authors would like to thank Oliver Jensen, Ian Jones and Timothy Waite for their advice and critical review of the manuscript; all AirPROM Consortium members for stimulating discussions at various stages of the study; and Davinder Kaur and Michael Biddle for assistance with the *in vitro* experiments.

Author contributions: I.L. Chernyavsky and B.S. Brook took part in mathematical model design; I.L. Chernyavsky performed numerical simulations; I.L. Chernyavsky, R.M. Saunders, G.E. Morris, F.R.A.J. Rose, S. Siddiqui, B.S. Brook and C.E. Brightling conceived the experimental model; R.M. Saunders and G.E. Morris conducted *in vitro* experiments; I.L. Chernyavsky, R.J. Russell and R.M. Saunders performed statistical data analysis; R. Berair, A. Singapuri, A.H. Mansur, P.H. Howarth, P. Dennison, R. Chaudhuri, S. Bicknell, S. Siddiqui and C.E. Brightling coordinated the clinical trial and undertook procedures; R.J. Russell, R. Berair and L. Chachi analysed patient biopsy data; I.L. Chernyavsky, R.J. Russell, R.M. Saunders, S. Siddiqui, B.S. Brook and C.E. Brightling interpreted the results and prepared the manuscript. All authors read and approved the final manuscript.

Support statement: The work was part supported by AirPROM 7th EU Framework grant 270194 (all authors), Medical Research Council (MRC) grant MR/N011538/1 (I.L. Chernyavsky), MRC grant MR/M004643/1 (B.S. Brook), Wellcome Trust Senior Fellowship WT082265 (C.E. Brightling) and by National Institute for Health (NIHR) Leicester Biomedical

Research Centre. The views expressed are those of the authors and not necessarily those of the NHS, the NIHR or the Department of Health. Funding information for this article has been deposited with the Crossref Funder Registry.

Conflict of interest: R.M. Saunders reports grants from 7th EU Framework, Wellcome Trust and National Institute for Health Research, during the conduct of the study. A.H. Mansur has received an educational grant for service support from AstraZeneca Pharmaceuticals, and received fees for talks and advisory group contribution and conference attendance from Novartis, GlaxoSmithKline, AstraZeneca, Napp Pharmaceuticals, Boehringer Ingelheim and others, outside the submitted work. P.H. Howarth reports grants from the European Union (AirPROM collaborative grant), during the conduct of the study. R. Chaudhuri reports being an advisory board member for GlaxoSmithKline, AstraZeneca, Teva Pharmaceutical Industries and Novartis and receiving educational grants for her institute from Novartis; receiving fees for speaking at meetings organised by GlaxoSmithKline, AstraZeneca, Chiesi and for attending international conferences sponsored by Novartis, Teva Pharmaceutical Industries, AstraZeneca and Boehringer Ingelheim. S. Siddiqui reports personal fees for advisory board participation from AstraZeneca and Boehringer Ingelheim, personal fees for advisory/consulting from Owlstone Nanotech and Mundipharma, speaker fees from Novartis, grants for imaging research in asthma from Napp Pharmaceuticals, and speaker fees from the European Respiratory Society, outside the submitted work. C.E. Brightling has received, paid to his institution, grants and consultancy fees from GlaxoSmithKline, Novartis, Chiesi, MedImmune/AstraZeneca, Boehringer Ingelheim, MSD Pharmaceuticals, PrEP Biopharm, Vectura, Teva Pharmaceutical Industries, Sanofi, Regeneron and Roche/Genentech. I.L. Chernyavsky reports research fellowship support from the European Commission (FP7 AirPROM) and a grant from Medical Research Council UK (New Investigator Research Grant), during the conduct of the study.

References

- 1 US FDA. Alair Bronchial Thermoplasty System. Summary of safety and effectiveness data. 2010. www.accessdata.fda.gov/cdrh_docs/pdf8/P080032b.pdf Date last accessed: April 24, 2018.
- 2 Wilhelm CP, Chipps BE. Bronchial thermoplasty: a review of the evidence. *Ann Allergy Asthma Immunol* 2016; 116: 92–98.
- 3 Seow CY, Fredberg JJ. Historical perspective on airway smooth muscle: the saga of a frustrated cell. *J Appl Physiol* 2001; 91: 938–952.
- 4 Mitzner W. Airway smooth muscle: the appendix of the lung. *Am J Respir Crit Care Med* 2004; 169: 787–790.
- 5 Zuyderduyn S, Sukkar MB, Fust A, et al. Treating asthma means treating airway smooth muscle cells. *Eur Respir J* 2008; 32: 265–274.
- 6 Janssen LJ. Airway smooth muscle as a target in asthma and the beneficial effects of bronchial thermoplasty. *J Allergy* 2012; 2012: 593784.
- 7 Laxmanan B, Hogarth DK. Bronchial thermoplasty in asthma: current perspectives. *J Asthma Allergy* 2015; 8: 39–49.
- 8 Danek CJ, Lombard CM, Dungworth DL, et al. Reduction in airway hyperresponsiveness to methacholine by the application of RF energy in dogs. *J Appl Physiol* 2004; 97: 1946–1953.
- 9 Cox G, Miller JD, McWilliams A, et al. Bronchial thermoplasty for asthma. *Am J Respir Crit Care Med* 2006; 173: 965–969.
- 10 Pavord ID, Cox G, Thomson NC, et al. Safety and efficacy of bronchial thermoplasty in symptomatic, severe asthma. *Am J Respir Crit Care Med* 2007; 176: 1185–1191.
- 11 Castro M, Rubin AS, Laviolette M, et al. Effectiveness and safety of bronchial thermoplasty in the treatment of severe asthma. *Am J Respir Crit Care Med* 2010; 181: 116–124.
- 12 Bellanti JA, Settupane RA. Bronchial thermoplasty: quo vadis? *Allergy Asthma Proc* 2015; 36: 240–240.
- 13 Pretolani M, Dombret M-C, Thabut G, et al. Reduction of airway smooth muscle mass by bronchial thermoplasty in patients with severe asthma. *Am J Respir Crit Care Med* 2014; 190: 1452–1454.
- 14 Chakir J, Haj-Salem I, Gras D, et al. Effects of bronchial thermoplasty on airway smooth muscle and collagen deposition in asthma. *Ann Am Thorac Soc* 2015; 12: 1612–1618.
- 15 Denner DR, Doering DC, Hogarth DK, et al. Airway inflammation after bronchial thermoplasty for severe asthma. *Ann Am Thorac Soc* 2015; 12: 1302–1309.
- 16 Pretolani M, Bergqvist A, Thabut G, et al. Effectiveness of bronchial thermoplasty in patients with severe refractory asthma: clinical and histopathologic correlations. *J Allergy Clin Immunol* 2017; 139: 1176–1185.
- 17 Berjano EJ Theoretical modeling for radiofrequency ablation: state-of-the-art and challenges for the future. *Biomed Eng Online* 2006; 5: 24.
- 18 Slebos D-J, Klooster K, Koegelenberg CFN, et al. Targeted lung denervation for moderate to severe COPD: a pilot study. *Thorax* 2015; 70: 411–419.
- 19 Jarrard J, Wizeman B, Brown R, et al. A theoretical model of the application of RF energy to the airway wall and its experimental validation. *Biomed Eng Online* 2010; 9: 81.
- 20 Dyrda P, Tazzeo T, DoHarris L, et al. Acute response of airway muscle to extreme temperature includes disruption of actin–myosin interaction. *Am J Respir Cell Mol Biol* 2011; 44: 213–221.
- 21 Kaur D, Gomez E, Doe C, et al. IL-33 drives airway hyper-responsiveness through IL-13-mediated mast cell: airway smooth muscle crosstalk. *Allergy* 2015; 70: 556–567.
- 22 Hollins F, Kaur D, Yang W, et al. Human airway smooth muscle promotes human lung mast cell survival, proliferation, and constitutive activation: cooperative roles for CADM1, stem cell factor, and IL-6. *J Immunol* 2008; 181: 2772–2780.
- 23 Dombret M-C, Alagha K, Boulet LP, et al. Bronchial thermoplasty: a new therapeutic option for the treatment of severe, uncontrolled asthma in adults. *Eur Respir Rev* 2014; 23: 510–518.
- 24 Berair R, Hartley R, Mistry V, et al. Associations in asthma between quantitative computed tomography and bronchial biopsy-derived airway remodelling. *Eur Respir J* 2017; 49: 1601507.
- 25 Boulet L-P, Laviolette M. Acute effects of bronchial thermoplasty: a matter of concern or an indicator of possible benefit to small airways? *Eur Respir J* 2017; 49: 1700029.
- 26 Purschke M, Laubach H-J, Anderson RR, et al. Thermal injury causes DNA damage and lethality in unheated surrounding cells: active thermal bystander effect. *J Invest Dermatol* 2010; 130: 86–92.

- 27 Kaur D, Saunders R, Berger P, *et al.* Airway smooth muscle and mast cell-derived CC chemokine ligand 19 mediate airway smooth muscle migration in asthma. *Am J Respir Crit Care Med* 2006; 174: 1179–1188.
- 28 Hinz B. The role of myofibroblasts in wound healing. *Curr Res Transl Med* 2016; 64: 171–177.
- 29 Gerarduzzi C, Di Battista JA. Myofibroblast repair mechanisms post-inflammatory response: a fibrotic perspective. *Inflamm Res* 2017; 66: 451–465.
- 30 Berair R, Brightling CE. Asthma therapy and its effect on airway remodelling. *Drugs* 2014; 74: 1345–1369.

Online Supplementary Material

In vitro, *in silico* and *in vivo* study challenges the impact of bronchial thermoplasty on acute airway smooth muscle mass loss

I.L. Chernyavsky*, R.J. Russell, R.M. Saunders, G.E. Morris, R. Berair, A. Singapuri, L. Chachi, A.H. Mansur, P.H. Howarth, P. Dennison, R. Chaudhuri, S. Bicknell, F.R.A.J. Rose, S. Siddiqui, B.S. Brook, C.E. Brightling

Supplementary Methods

A model of Joule heating and bioheat transfer

To simulate the thermal impact of bronchial thermoplasty, we employ a 2D mathematical model that couples electric current generated by the electrodes (with integrated temperature control feedback) and heat transfer in the airway wall and surrounding parenchymal tissue. Figure S1 illustrates the relationship between the *in vitro*, *in silico* and *in vivo* methodologies used to assess the direct acute impact of bronchial thermoplasty on airway wall composition.

Following established models of radiofrequency thermal ablation [S1–5], we use quasi-electrostatic current conservation

$$\nabla \cdot (\sigma \nabla \varphi) = 0, \quad (1)$$

for electric potential φ , and the bioheat transfer equation for temperature T in the airway lumen, wall

* Author for correspondence (Igor.Chernyavsky@manchester.ac.uk).

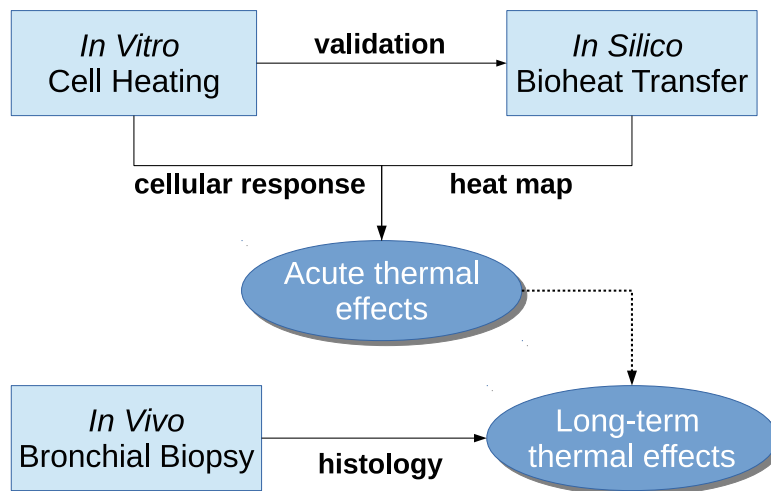


Figure S1: An overview of the approaches used in the study, in the context of acute and long-term thermal effects.

and parenchymal tissue:

$$c \rho \frac{\partial T}{\partial t} = \nabla \cdot (\kappa \nabla T) + Q_{\text{joule}} - Q_{\text{diss}}, \quad (2)$$

where σ and κ are the electric and thermal conductivities respectively, c is the specific heat capacity and ρ is the medium density (see Table S1); $Q_{\text{joule}} = \sigma |\varphi|^2$ is the Joule heating source and $Q_{\text{diss}} = Q_{\text{perf}} + Q_{\text{evap}}$ is the heat dissipation due to blood perfusion and evaporative cooling. Perfusion cooling is assumed to be the only volumetric sink in the airway wall:

$$Q_{\text{perf}}^{\text{wall}} \approx \alpha q_{\text{perf}} (T - T_0), \quad (3)$$

where $T_0 = 37^\circ\text{C}$ is the reference body temperature, $q_{\text{perf}} = c_b \rho_b \omega_b \sim 10^4 - 10^5 \text{ W}/(\text{K}\cdot\text{m}^3)$ is the perfusion rate (ω_b) times blood density (ρ_b) and specific heat capacity (c_b) [S1], and $\alpha = 0.5$ is the wall perfusion factor that accounts for partial vascularisation. In parenchyma, we take $Q_{\text{perf}}^{\text{par}}$ identical to (3), with perfusion factor α set to 1.

The heat carried away with evaporation into alveolar space in the parenchyma can be approximately described (see eqn. (12) in the Appendix) by

$$Q_{\text{evap}}^{\text{par}} \approx \frac{\phi_a}{1 - \phi_a} \frac{4\pi}{3} k_a \Delta H [C_s(T) - C(T_0)], \quad (4)$$

where $C_s(T)$ is the saturated concentration of water vapour at given temperature, ΔH is the specific heat (enthalpy) of vaporisation of water, ϕ_a is the parenchymal porosity, and $k_a \sim 10^{-1} \text{ s}^{-1}$ is the mean vapour evacuation rate from an alveolus to trachea. k_a is estimated by comparing the diffusive and advective timescales for moisture transport in a typical pathway from an alveolus to trachea, which consists of about 25 cm of conductive and 1 cm of diffusive portions [S6]. Saturated water vapour concentration in air C_s (kg/m^3) exhibits exponential dependence on temperature T ($^\circ\text{C}$), which is approximated (in the range of -50 to 100°C) by $C_s(T) \approx m (T + 273)^{k_1} 10^{k_3 + k_2/(T+273)}$ for $m = 0.21668$, $k_1 = -5.9283$, $k_2 = -2937.4$, $k_3 = 23.5518$ [S7]. Reference material parameter values are given in Tables S1 and S3. Similarly, the evaporation-aided cooling into the luminal space is described by a flux across the luminal surface

$$\kappa_{\text{wall}} \mathbf{n} \cdot \nabla T = D_v \Delta H \mathbf{n} \cdot \nabla C \approx 2 D_v \Delta H [C_s(T) - \eta C_s(T_0)]/R_0, \quad (5)$$

where D_v is the diffusivity of water vapour, $\eta = 0.95$ is the relative humidity of the luminal airspace and R_0 is the inner airway wall radius; here we also assumed, following [S8], a parabolic profile of vapour concentration in the lumen, with vapour concentration of $C_s(T)$ and $\eta C_s(T_0)$ on the luminal surface and at the centre of an airway respectively.

The system of equations (1)–(2) is complemented by boundary conditions that set body temperature ($T = T_0$) and zero electric potential ($\varphi = 0$) at the outer parenchymal boundary, and ensure continuity of temperature, electric potential, thermal flux and electric current at all the interfaces. The electric potential at the electrode surface is given by $\varphi|_{\text{electrode}} = V(t)$ that obeys the electrode voltage control equation

$$\frac{dV}{dt} = k_i (T_1 - T_e) - k_p \frac{dT_e}{dt}, \quad V|_{t=0} = 0, \quad (6)$$

where T_e is the temperature at the electrode inward-facing luminal surface and T_1 is the target temperature of 65°C ; the integral $k_i = 20 \text{ V}/(\text{K}\cdot\text{s})$ and proportional $k_p = 16 \text{ V}/\text{K}$ reference control parameters

	electrode	luminal air	wall tissue	parenchyma
Electrical conductivity (σ , S/m) ^a	10^6	$10^{-16} - 10^{-15}$	0.4	0.15
Thermal conductivity (κ , W/(m · K)) ^b	16	3×10^{-2}	0.5	0.45
Specific heat capacity (c , J/(kg · K)) ^c	5×10^2	10^3	3.5×10^3	1.6×10^3
Density (ρ , kg/m ³) ^d	8×10^3	1	10^3	2×10^2
Thermal diffusivity ($D = \kappa/(\rho c)$, m ² /s)	4×10^{-6}	3×10^{-5}	1.4×10^{-7}	1.4×10^{-6}
Water vapour diffusivity in air (D_v , m ² /s)		2.7×10^{-5} [S8]		
Latent heat of vaporisation (ΔH , J/kg)		2.4×10^6 [S8]		

^a from [S1, S11], ^{b, c, d} compiled from [S1, S8, S12, S13].

Table S1: Material properties of the lung (at ca. 37°C and normal atmospheric pressure).

are chosen so that the target temperature is reached in about 2 seconds within specified maximum power characteristics [S9].

As a reference model geometry we consider a concentric circular cross-section of an airway with the luminal radius of $R_0 = 2.2$ mm, airway wall thickness-to-radius ratio of $h/R_0 = 0.6$ and outer parenchymal radius of 50 mm. Each of the four electrodes has the dimensions of 0.13×0.33 mm [S9, S10].

***In vitro* heating of human primary ASM and epithelial cells and bronchial epithelial cell-line**

Primary ASM cells derived from ASM bundles isolated from bronchial biopsies and used from passage 2 – 6, and primary epithelial cells derived from bronchial brushings were cultured as described previously [S14]. The study was approved by the Leicestershire Research Ethics Committee (REC 08/H0406/189). Informed consent was obtained from all subjects. The immortalized human bronchial epithelial cell-line (hBEC) was obtained from the LGC Standards cell bank (Middlesex, UK).

Prior to heating, primary ASM and epithelial cells and hBECs were grown to confluence in 24- or 6-well plates. Media was heated to specified temperatures in Eppendorf tubes in a heat block (Accublock™ Digital Dry Bath, Labnet International Inc., Edison, USA). Cell medium was aspirated and replaced with heated medium for 10 seconds before being aspirated off, replaced with fresh medium and returned to the 5% CO₂ incubator at 37°C. To account for loss of heat from the media over the 10 second period, the mean temperature the cells were exposed to over 10 seconds, and the temperature of the media at the end of the 10 second period were assessed in both 24- and 6-well plates (see Table S4 below). This showed that the media heated to 65°C had a mean temperature over the 10 seconds of 58 – 59°C in both the 24- and 6-well plates.

In order to eliminate possible artefacts in the heating response related to cell type, the survival response of primary epithelial cells versus the transformed hBEC cell line following heating was compared. We found acute thermal effects to be similar in both cultures (see Table S2), with the greatest response to heating in both primary and transformed epithelial cells occurring with media heated to 65°C (Table S2); thus hBECs were used for further experimentation. The number of remaining

Viable epithelial cells 24 h post-heating (% viability at day 0)				
Temperature media heated to, °C	hBEC cell line (n=7)	<i>p</i> -value	Primary cells (n=3)	<i>p</i> -value
37	92 ± 4	—	97 ± 7	—
50	101 ± 6	0.7	96 ± 5	1
55	98 ± 6	0.9	92 ± 6	0.9
60	91 ± 6	1	77 ± 4	0.07
65	45 ± 7 *	10 ⁻⁴	20 ± 4 *	10 ⁻⁴

Table S2: Viability of primary epithelial cells versus hBEC cell line assessed with PrestoBlue. Data are presented as mean ± SEM; * indicates $p < 0.001$ vs. 37°C, using a one-way ANOVA with Dunnett’s multiple comparisons test and *p*-value adjustment.

adherent viable primary ASM cells or hBECs at specified time points over a 2 week period was indirectly determined by measuring cell metabolic activity using PrestoBlue® (Thermo Fisher Scientific, Warrington, UK) according to the manufacturer’s instructions and confirmed at 24 – 48 hours, 1 week and 2 weeks by cell counting in independent experiments.

In order to assess the survival status of the cells that remained adhered to the plates 24 h after heating, the percentage of the ASM or hBEC cell population undergoing apoptosis or necrosis post-heating was determined by using the Alexa Fluor® 488 Annexin V / Dead Cell Apoptosis kit (Thermo Fisher Scientific, Warrington, UK) according to the manufacturer’s instructions as described previously [S15]. Samples were analysed on a flow cytometer (FC 500; Beckman Coulter, High Wycombe, UK), using *Weasel*™ software (Frank Battye, Melbourne, Australia). Fluorescence emission was collected at 530 nm (Annexin V) and > 575 nm (propidium iodide) and the percentage of the apoptotic and necrotic cells derived respectively.

***In vivo* response to BT**

Bronchial biopsies were obtained from 14 subjects before and after BT. All subjects had severe asthma as defined by ATS/ERS guidelines, and underwent BT as part of their clinical care at one of four UK specialist centres (Leicester, Glasgow, Southampton and Birmingham). Subjects underwent clinical assessments whilst stable prior to BT and about six weeks after the final treatment. The study was approved by the Leicestershire Research Ethics Committee (REC 13/EM/0068). Informed written consent was obtained from all subjects.

BT was performed as per manufacturer’s guidelines over three staged treatment sessions in the following order: right lower lobe (RLL); left lower lobe (LLL), and both right and left upper lobes (RUL, LUL). The right middle lobe was not treated due to the risk of airway collapse and ‘right middle lobe syndrome’ [23]. Biopsies (two to five) were obtained from the untreated RUL and then the treated RLL segmental and subsegmental airways at the first and second BT sessions respectively. It was recommended that each BT session be separated by 3 – 4 weeks.

Biopsies were embedded in paraffin. Four micrometre sections were cut and stained with Haemato-

xylin and Eosin or anti- α -smooth muscle actin (α -SMA, clone 1A4, Dako, UK). Biopsies were assessed by a single observer (RJR) blinded to clinical characteristics, using ZEN 2012 (Carl Zeiss AG, Germany). ASM content was determined as percentage of the total biopsy area. Epithelial integrity was assessed by measuring the length of intact, damaged and denuded epithelium as a percentage of the reticular basement membrane length. Myofibroblasts (isolated α -SMA positive stained cells in the lamina propria that were neither located as part of the ASM-bundle nor as vascular smooth muscle cells adjacent to vessels) were counted and expressed as cells per mm^2 of lamina propria.

Statistical analysis

Data was analysed in GraphPad Prism[®] 7.0 (San Diego, California, USA) and R Project 3.2.4, using parametric and non-parametric tests as indicated below. Confidence intervals for the medians of cell counts were estimated using the bootstrap percentile method (R boot package). The following tests for difference in medians were used: Kruskal–Wallis rank test with Dunns post-test for cell viability assays, Wilcoxon paired test with Benjamini–Hochberg–Yekutieli post-hoc p -value adjustment for direct and indirect cell counts. Assuming a mean \pm standard deviation ASM mass of $25 \pm 15\%$ [S16], $N = 14$ subjects were required to observe an absolute reduction of 10% ASM mass using a one-tailed paired test with 80% power at the significance level of 0.05. Features of baseline and follow-up biopsies were compared using paired Wilcoxon signed-rank test. Pre-BT ASM mass, epithelial integrity and myofibroblast numbers in the lamina propria and their change post-BT were compared with change in Asthma Control Questionnaire-6 (ACQ6) and Asthma Quality of Life Questionnaire (AQLQ) and between responder and non-responder groups (minimal important clinical difference 0.5; responder defined as ≥ 1.0 improvement as substantial effects were previously observed with sham-procedure [S17]). A p -value of < 0.05 was considered statistically significant.

Supplementary Results

In silico model sensitivity analysis

To assess relative contribution of parameters of the mathematical model, we performed local sensitivity analysis [S18]. Table S3 reports relative sensitivity $\frac{\Delta f/f}{\Delta p/p}$ in model prediction f , resulting from a moderate change in parameter value p . For example, a 10% change in electrical wall conductivity, σ , that results in approximately 1% change in the average wall temperature, $\langle T \rangle$, gives a relative sensitivity of $\langle T \rangle$ with respect to σ of about 0.1.

The analysis suggests relative insensitivity of the model to the material properties and heating control parameters (except the target temperature, which is fixed to high precision). However, BT heating efficiency (in terms of both $\langle T \rangle$ and the fraction of the wall ϕ_{65} heated above 65°C) is shown to be strongly dependent on the airway inner radius and wall thickness (Table S3).

We also further explore the radial distribution of the heat generated by the BT in an airway wall (see Fig. 2 of the main text) by computing heated wall area fractions as a function of the averaging distance from the airway lumen (Figure S2). In doing so we quantify the amount of energy delivered to the inner portion to the wall (small distance from the lumen in Figure S2), compared to the thermal energy averaged over the entire airway wall area (large distance from the lumen). Note that there is a

	Parameter	Reference value (p)	Relative sensitivity of mean temperature $\langle T \rangle(p)$	Relative sensitivity of top-heated area fraction $\phi_{65}(p)$
Geometric	Luminal radius, mm	2.2	-0.33	-7.9*
	Outer wall radius, mm	3.52	-0.25	-7.2*
	Electrode breadth, mm	0.33	0.09	2.6*
	Electrode thickness, mm	0.13	0.04	1.2
Physiologic	Wall electrical conductivity σ , S/m	0.4	0.10	1.6
	Parenchymal electric conductivity σ , S/m	0.15	-0.10	-1.4
	Wall thermal conductivity κ , W/(m·K)	0.5	0.10	0.9
	Wall thermal inertia $c\rho$, J/(K·m ³)	3.5×10^6	-0.05	-0.5
	Parenchymal thermal inertia $c\rho$, J/(K·m ³)	3.8×10^5	-0.03	-0.4
	Reference body temperature T_0 , °C	37	0.11	1.2
	Parenchymal porosity ϕ_a	0.8	-0.08	-1.0
	Alveolar vapour evacuation rate k_a , s ⁻¹	0.1	-0.01	-0.2
	Perfusion cooling rate q_{perf} , W/(K·m ³)	0.1	-0.01	-0.2
	Control	Time of heating t_0 , s	10	0.09
Target temperature T_1 , °C		65	0.87	65.2*
Proportional feedback control k_p , V/K		16	-0.01	-0.1

Table S3: Local sensitivity analysis of model parameters (showing only the parameters with relative sensitivity of $\langle T \rangle$ of magnitude 0.01 and above). * indicates parameters important for the simulated thermal impact of BT.

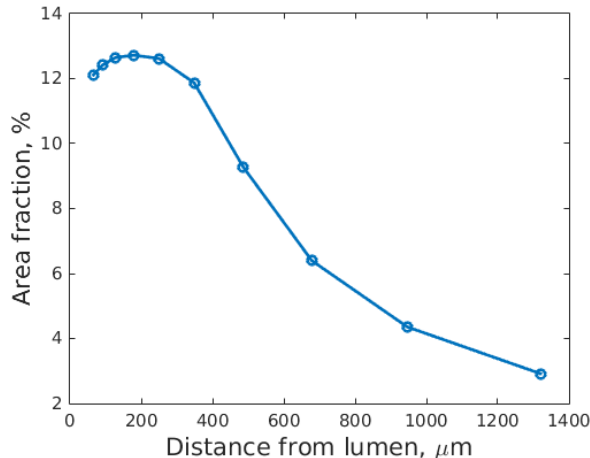


Figure S2: Radial-averaged fraction of airway wall heated to or above 65°C as a function of the distance from the lumen.

maximum in Figure S2, corresponding to the highest proportion of the hot spots, close to the luminal surface but not at the surface itself due to evaporative cooling effects and ‘blanket’ heating between the electrode and inner parenchyma (which is more resistant to electric current and, at the same time, causes faster redistribution of the generated heat, owing to higher thermal diffusivity; see Table S1).

Validation of *in silico* model of *in vitro* cooling

To account for loss of heat from the media and to assess temperature variation over time during the *in vitro* heating experiments (see Methods for more details), we performed controlled cooling experiments for the range of temperatures used in *in vitro* cell heating. Table S4 shows the mean temperature the cells were exposed over the 10 second period and the minimal temperature of the media at the end of this period in both 24- and 6-well plates. We used the *in vitro* cooling dataset to validate the mathematical model of bioheat transfer (2)–(5) modified to match the multi-well plate geometry and material properties.

The cooling model is given by the heat transfer equation (2), with heat sources and sinks Q set to zero. The axisymmetric model geometry (with coordinates (r,z) ; see Fig. S3A) is divided into the domains of polystyrene plate walls (w), the liquid medium (m) and the air above the medium (a), which are characterised by the material properties of Table S1, complemented by the polystyrene wall and medium thermal conductivities $\kappa_m = 0.6$ and $\kappa_w = 0.2 \text{ W}/(\text{m} \cdot \text{K})$; the wall and medium densities $\rho_w = 1.1 \times 10^3$ and $\rho_m = 10^3 \text{ kg}/\text{m}^3$; and the wall and medium specific heat capacities $c_w = 2 \times 10^3$ and $c_m = 4 \times 10^3 \text{ J}/(\text{kg} \cdot \text{K})$ [S19]. According to the manufacturer’s specifications, Corning[®] Falcon[®] and Costar[®] 6-well culture plates have the base radius of a single well of approximately $a = 17.4 \text{ mm}$, the height of about $h = 18 \text{ mm}$ and the base wall thickness of about $d = 1.6 \text{ mm}$. Taking the volume of 1.5 ml for the medium used in the *in vitro* tests, gives the medium layer depth of approximately $\delta = 1.6 \text{ mm}$.

We require the continuity of concentration and fluxes at all internal interfaces and complement

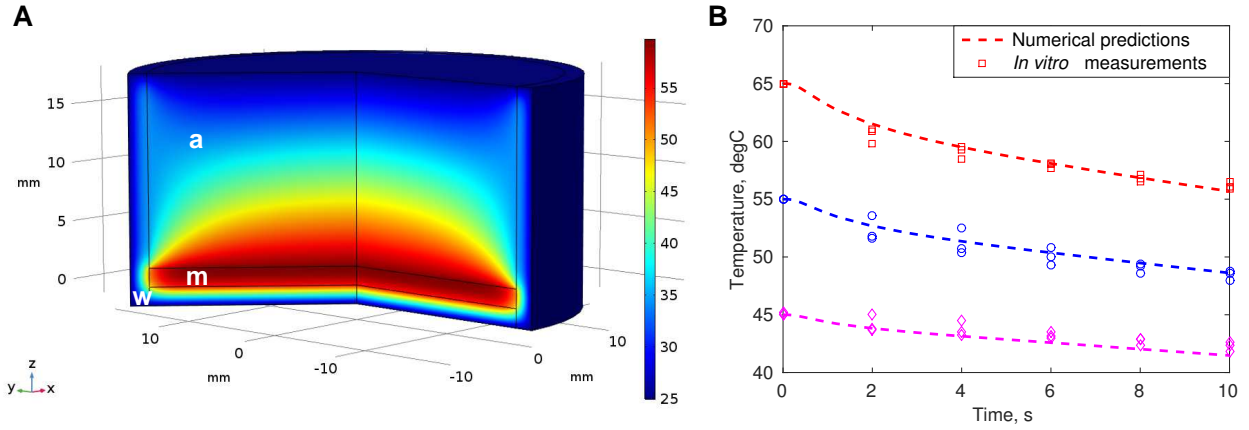


Figure S3: Comparison of *in silico* and *in vitro* models of heat transfer in a 6-well plate. (A) Temperature distribution in the medium (m), plate wall (w) and air (a) at 5 seconds after the initial medium temperature of 65°C. (B) Associated cooling curves predicted by the mathematical model (at mid-depth $z = \delta/2$, $r = 0$; dashed lines) and measured at varying positions *in vitro* (symbols).

	24-well plate (0.5 ml medium; n=3)		6-well plate (1.5 ml medium; n=3)	
Temperature media heated to, °C	Temperature after 10 s, °C	Mean temperature over 10 s, °C	Temperature after 10 s, °C	Mean temperature over 10 s, °C
37	36.1 ± 0.6	36.4 ± 0.4	36.3 ± 0.1	36.8 ± 0.1
45	42.7 ± 0.1	43.4 ± 0.1	42.1 ± 0.4	43.5 ± 0.2
50	46.0 ± 0.2	47.3 ± 0.02	44.0 ± 1.6	46.5 ± 1.0
55	49.6 ± 0.3	51.2 ± 0.2	48.4 ± 0.3	51.0 ± 0.3
60	52.7 ± 0.1	55.0 ± 0.1	52.3 ± 0.9	55.6 ± 0.6
65	54.9 ± 0.3	58.0 ± 0.2	56.1 ± 0.2	59.3 ± 0.2

Table S4: Experimental measurements of mean and minimum temperatures of media *in vitro* over the period of 10 seconds. Data are presented as mean ± SEM.

heat transfer by adding diffusion of the water vapour in the air above the medium

$$\partial_t C = D_v \nabla^2 C \quad (7)$$

and by balancing the direct and evaporation-mediated heat fluxes on the free surface ($z = \delta$), coupled with saturated vapour concentration C_s , given by

$$\kappa_m \mathbf{n} \cdot \nabla T = \kappa_a \mathbf{n} \cdot \nabla T + D_v \Delta H \mathbf{n} \cdot \nabla C, \quad C = C_s(T). \quad (8)$$

Since the timescales for diffusion in the air, polystyrene wall and liquid medium for the given geometry are of the same order of magnitude (~ 10 s), the model cannot be reduced further without loss of accuracy.

Finally, we set room temperature outside the plate and initially inside the air layer ($T_a|_{t=0} = 25^\circ\text{C}$), assume zero moisture level at the upper boundary ($C|_{z=h} = 0$) and the initial temperature of the plate wall equal to the incubator temperature ($T_w|_{t=0} = 37^\circ\text{C}$).

Figure S3(A) illustrates a heat map of the coupled moisture-heat diffusion model solved in COMSOL Multiphysics[®] 5.3, 5 seconds after the start of the experiment. The distribution of temperatures in the medium is fairly uniform for the 6-well plate, but is more heterogeneous for a smaller 24-well plate (not shown) due to a thicker layer of the medium. The comparison of the numerically-predicted transient cooling, fitted to the experimental data at 60°C (via thermal properties of the plate wall), demonstrates good agreement over a wide range of temperatures (Figure S3B and Table S4). This approach therefore contributes to validating the heat-transfer component of the mathematical thermoplasty model. Nonetheless, there remain experimental, physical and geometrical uncertainties in the model parameters. The predictions of the mathematical model are thus intended to provide a qualitative rather than quantitative insight into the impact of BT.

Appendix: Evaporative flux into alveolar space

Below we estimate the quasi-steady evaporation flux into a sphere with slow evacuation of vapour, which is used to approximate the corresponding cooling term in the bioheat transfer equation (2).

Provided that the heat loss from evaporation into the alveolar space is limited by the vapour evacuation timescale, we consider the steady state transport of moisture

$$\frac{D_v}{r^2} \frac{\partial}{\partial r} \left(r^2 \frac{\partial C}{\partial r} \right) - \varepsilon \gamma (C - C_0) = 0, \quad 0 \leq r < a \quad (9a)$$

where $k_a = O(\varepsilon) \equiv \varepsilon \gamma$ is the evacuation rate, with $\gamma = O(1)$, $\varepsilon \ll 1$, with corresponding boundary conditions

$$C|_{r=a} = C_s(T), \quad |C|_{r \rightarrow 0} < \infty \quad (9b)$$

Expanding C into asymptotic series $C \approx C^{(0)} + \varepsilon C^{(1)} + \dots$, we find, at leading order, $C^{(0)} = A/r + B$ for some constants A, B , which reduces to $C^{(0)} = C_s(T)$ after applying the boundary constraints (9b).

The correction $C^{(1)}$ obeys

$$\frac{D_v}{r^2} \frac{d}{dr} \left(r^2 \frac{dC^{(1)}}{dr} \right) - \varepsilon \gamma (C^{(0)} - C_0) = 0, \quad (10)$$

and, by applying again the boundary conditions (9b) and using the concentration-independence of the leading order solution, we can express the correction as $C^{(1)} = \gamma (C_s - C_0) (r^2 - a^2)/(6 D_v)$, and thus the evaporative flux j_v at the alveolar surface can be approximated by

$$j_v = D_v \left. \frac{\partial C}{\partial r} \right|_{r=a} \approx \varepsilon D_v \left. \frac{\partial C^{(1)}}{\partial r} \right|_{r=a} = \frac{a k_a}{3} (C_s(T) - C_0). \quad (11)$$

The volumetric heat loss density is thus given by multiplying (11) by relative volumetric density of alveolar space $\frac{\phi_a}{1-\phi_a}$, the latent heat of evaporation ΔH , surface area of a single alveolus $4\pi a^2$, the total number of alveoli $N \sim L^3/a^3$ and dividing by the lung volume L^3 :

$$Q_{\text{evap}} = \frac{\phi_a}{1-\phi_a} (4\pi/a) \Delta H j_v \approx \frac{\phi_a}{1-\phi_a} \frac{4\pi}{3} k_a \Delta H (C_s(T) - C_0). \quad (12)$$

References

- S1. Jarrard J, Wizeman B, Brown R, Mitzner W. A theoretical model of the application of RF energy to the airway wall and its experimental validation. *Biomed Eng Online* 2010;9:81.
- S2. Ryan TP, Patel SJ, Morris R, Hoopes PJ, Bergeron JA, Mahajan R. Three-dimensional finite element simulations of vertebral body thermal treatment. In: *Proc SPIE*, vol. 5698, Thermal Treatment of Tissue: Energy Delivery and Assessment III; 2005. pp. 137–155.
- S3. Humphries S, Johnson K, Rick K, Liu Zj, Goldberg SN. Three-dimensional finite-element code for electrosurgery and thermal ablation simulations. In: *Proc SPIE*, vol. 5698, Thermal Treatment of Tissue: Energy Delivery and Assessment III; 2005. pp. 181–194.
- S4. Chang I, Nguyen U. Thermal modeling of lesion growth with radiofrequency ablation devices. *Biomed Eng Online* 2004;3:27.
- S5. Shahidi AV, Savard P. A finite element model for radiofrequency ablation of the myocardium. *IEEE Trans Biomed Eng* 1994;41:963–968.
- S6. Ochs M, Burri PH, Gil J, Weibel ER. *General Thoracic Surgery*, vol. 1, ch. Ultrastructure and Morphometry of the Human Lung. 7th ed. Lippincott Williams & Wilkins; 2009. pp. 265–300.
- S7. Parish OO, Putnam TW. *Equations for the determination of humidity from dewpoint and psychrometric data*. NASA Technical Note D-8401, Dryden Flight Research Centre; 1977.
- S8. Tawhai MH, Hunter PJ. Modeling water vapor and heat transfer in the normal and the intubated airways. *Ann Biomed Eng* 2004;32:609–622.
- S9. *Alair Bronchial Thermoplasty System*. Summary of Safety and Effectiveness Data P080032, US FDA; 2010.
- S10. Danek C, Biggs M, Burger K, Loomas B, Keast T, Haugaard D. Modification of airways by application of energy. US Patent US9033976 B2; 2015.
- S11. Pawar SD, Murugavel P, Lal DM. Effect of relative humidity and sea level pressure on electrical conductivity of air over Indian Ocean. *J Geophys Res* 2009;114:D02205.
- S12. Haynes W. *CRC Handbook of Chemistry and Physics*. 95th ed. Taylor & Francis; 2014.
- S13. Saidel GM, Kruse KL, Primiano FP Jr. Model simulation of heat and water transport dynamics in an airway. *J Biomech Eng* 1983;105:188–193.
- S14. Kaur D, Gomez E, Doe C, Berair R, Woodman L, Saunders R, Hollins F, Rose FR, Amrani Y, May R, Kearley J, Humbles A, Cohen ES, Brightling CE. IL-33 drives airway hyper-responsiveness through IL-13-mediated mast cell: airway smooth muscle crosstalk. *Allergy* 2015; 70:556–567.

- S15. Hollins F, Kaur D, Yang W, Cruse G, Saunders R, Sutcliffe A, Berger P, Ito A, Brightling CE, Bradding P. Human airway smooth muscle promotes human lung mast cell survival, proliferation, and constitutive activation: cooperative roles for CADM1, stem cell factor, and IL-6. *J Immunol* 2008;181:2772–80.
- S16. Berair R, Hartley R, Mistry V, Sheshadri A, Gupta S, Singapuri A, Gonem S, Marshall RP, Sousa AR, Shikotra A, Kay R, Wardlaw A, Bradding P, Siddiqui S, Castro M, Brightling CE. Associations in asthma between quantitative computed tomography and bronchial biopsy-derived airway remodelling. *Eur Respir J* 2017;49:1601507.
- S17. Castro M, Rubin AS, Laviolette M, Fiterman J, De Andrade Lima M, Shah PL, Fiss E, Olivenstein R, Thomson NC, Niven RM, Pavord ID, Simoff M, Duhamel DR, McEvoy C, Barbers R, ten Hacken NH, Wechsler ME, Holmes M, Phillips MJ, Erzurum S, Lunn W, Israel E, Jarjour N, Kraft M, Shargill NS, Quiring J, Berry SM, Cox G. Effectiveness and safety of bronchial thermoplasty in the treatment of severe asthma. *Am J Respir Crit Care Med* 2010;181:116–124.
- S18. van Leeuwen IM, Byrne HM, Jensen OE, King JR. Elucidating the interactions between the adhesive and transcriptional functions of β -catenin in normal and cancerous cells. *J Theor Biol* 2007;247:77–102.
- S19. MatWeb. Online database of engineering materials; 2017. <http://www.matweb.com> (accessed 30 Nov 2017).